AMERICAN SOCIETY FOR MICROBIOLOGY | Antimicrobial Agents and Chemotherapy®

The *Acinetobacter* Outer Membrane Contains Multiple Specific Channels for Carbapenem β-Lactams as Revealed by Kinetic Characterization Analyses of Imipenem Permeation into *Acinetobacter baylyi* Cells

Jorgelina Morán-Barrio, María M. Cameranesi, Verónica Relling, Adriana S. Limansky, Luciano Brambilla, Alejandro M. Viale

Instituto de Biología Molecular y Celular de Rosario (IBR), Departamento de Microbiología, Facultad de Ciencias Bioquímicas y Farmacéuticas, CONICET, Universidad Nacional de Rosario (UNR), Rosario, Argentina

ABSTRACT The number and type of outer membrane (OM) channels responsible for carbapenem uptake in *Acinetobacter* are still not well defined. Here, we addressed these questions by using *Acinetobacter baylyi* as a model species and a combination of methodologies aimed to characterize OM channels in their original membrane environment. Kinetic and competition analyses of imipenem (IPM) uptake by *A. baylyi* whole cells allowed us to identify different carbapenem-specific OM uptake sites. Comparative analyses of IPM uptake by *A. baylyi* wild-type (WT) cells and Δ*carO* mutants lacking CarO indicated that this OM protein provided a carbapenem uptake site displaying saturable kinetics and common binding sites for basic amino acids compatible with a specific channel. The kinetic analysis uncovered another carbapenem-specific channel displaying a somewhat lower affinity for IPM than that of CarO and, in addition, common binding sites for basic amino acids as determined by competition studies. The use of *A. baylyi* gene deletion mutants lacking OM proteins proposed to function in carbapenem uptake in *Acinetobacter baumannii* indicated that CarO and OprD/OccAB1 mutants displayed low but consistent reductions in susceptibility to different carbapenems, including IPM, meropenem, and ertapenem. These two mutants also showed impaired growth on L-Arg but not on other carbon sources, further supporting a role of CarO and OprD/OccAB1 in basic amino acid and carbapenem uptake. A multiple-carbapenem-channel scenario may provide clues to our understanding of the contribution of OM channel loss or mutation to the carbapenem-resistant phenotype evolved by pathogenic members of the *Acinetobacter* genus.

KEYWORDS *Acinetobacter*, antibiotic resistance, basic amino acid channels, carbapenem outer membrane channels, carbapenem resistance, Gram-negative bacteria, outer membrane proteins

Received 10 August 2016 **Returned for modification** 17 September 2016 **Accepted** 28 December 2016

Accepted manuscript posted online 9 January 2017

Citation Morán-Barrio J, Cameranesi MM, Relling V, Limansky AS, Brambilla L, Viale AM. 2017. The *Acinetobacter* outer membrane contains multiple specific channels for carbapenem β-lactams as revealed by kinetic characterization analyses of imipenem permeation into *Acinetobacter baylyi* cells. Antimicrob Agents Chemother 61:e01737-16. https://doi.org/10.1128/AAC.01737-16.

Address correspondence to Alejandro M. Viale, viale@ibr-conicet.gov.ar.

The genus *Acinetobacter* (family *Moraxellaceae*, order *Pseudomonadales*, class *Gammaproteobacteria*) is composed of Gram-negative aerobic bacteria ubiquitously found in the environment and endowed with a large spectrum of metabolic capabilities (1–5). Some *Acinetobacter* members, such as those composing the *A. calcoaceticus*/*A. baumannii* (Acb) complex, are frequently associated with opportunistic nosocomial infections, with the responsible lineages generally displaying multidrug-resistant (MDR) phenotypes (3, 4). Infectious *Acinetobacter* lineages have shown an outstanding ability to rapidly evolve resistance when subjected to new antimicrobial challenges, and a

most worrisome problem at present is the worldwide emergence of additional resistance to the last therapeutic options, such as broad-spectrum carbapenem β-lactams (3–6).

Carbapenem resistance results from an interplay of different factors, including decreased outer membrane (OM) permeability, overproduction of endogenous or acquired carbapenemases, efflux pumps, and even modification of metabolic networks (3, 7–10). The carbapenems traverse the OM barrier through β-barrel protein channels that are normally employed for the uptake of low-molecular-mass hydrophilic nutrients, of which two types have been described: general and specific (7, 8). General channels lack measurable affinities for permeating compounds, as exemplified by the OmpF/C "fast" porins of the *Enterobacteriaceae*. On the contrary, specific channels are endowed with low-affinity binding sites for particular substrates and are thus generally characterized by substrate saturation kinetics in the submillimolar range and competition for uptake between substrates sharing the same binding site(s) (7, 8). As expected, the introduction of carbapenem therapy in the 1980s was rapidly followed by the emergence of Gram-negative pathogen lineages displaying channel mutations resulting in reduced OM antibiotic permeability (7, 8).

The members of the genus *Acinetobacter*, as for *Pseudomonas*, lack "fast" general porins and depend mainly on specific channels for nutrient uptake (7, 8). Although this absence may explain their general intrinsic resistance to most β-lactams, *Acinetobacter* spp. are generally highly susceptible to the carbapenems, indicating the use of specific OM channels by these antibiotics (3, 6, 8, 9, 11, 12). The identification of such channels has remained elusive, and a number of OM proteins, including CarO (13–15), the Omp33/36 protein (16), and a 43-kDa protein designated OprD (17), have been proposed as candidates on the basis of their loss in carbapenem-resistant *Acinetobacter baumannii* clinical strains. However, both the role of these OM proteins in carbapenem uptake and the contribution of their loss or mutation to the carbapenem-resistant phenotype, particularly in strains displaying another mechanism(s) of resistance, have been the subjects of controversies (3, 15, 18–34).

A possible explanation for the difficulties in identifying specific channels is the existence in the *Acinetobacter* OM of several independent sites allowing significant carbapenem influx (12, 24). In such a multiple-carbapenem-channel scenario, carbapenem resistance may rely mainly on a more robust mechanism of resistance rather than on reductions in OM permeability resulting from the simultaneous loss of different uptake sites, especially if these sites play important roles in nutrient uptake. In cells already possessing a main mechanism of resistance, however, channel mutations promoting even small reductions in carbapenem uptake may still be selected under particular conditions, such as low antibiotic concentrations in which small differences in permeation may favor the growth of the mutants over that of the parental cells (8, 35). It follows that a better understanding of the channels involved in carbapenem uptake in the *Acinetobacter* OM may shed light on the contributions of their loss to resistance and therefore to the adaptation to the clinical environment.

We addressed here the above questions by employing whole cells and a combination of biochemical, genetic, and microbiological procedures aimed at a more quantitative characterization of OM channels in their original cell milieu in accordance with procedures described for other Gram-negative bacterial species (7, 8, 12, 36–39). We selected *Acinetobacter baylyi* for this purpose, given its ample use as a model for the study of the general physiological aspects of the genus *Acinetobacter* (1, 2, 5, 11, 40–42). In short, we characterized the kinetics of imipenem (IPM) diffusion into intact *A. baylyi* cells by coupling the influx of this carbapenem with a rapid sink hydrolysis by a periplasmic VIM carbapenemase. We also characterized the role of CarO in this uptake by conducting a similar analysis with an *A. baylyi* mutant lacking the *carO* gene (Δ*carO*). The studies presented here revealed different specific channels allowing for significant IPM influx in the *Acinetobacter* OM, indicated that CarO is involved in this uptake, showed that basic amino acids compete with IPM for uptake through both CarO and

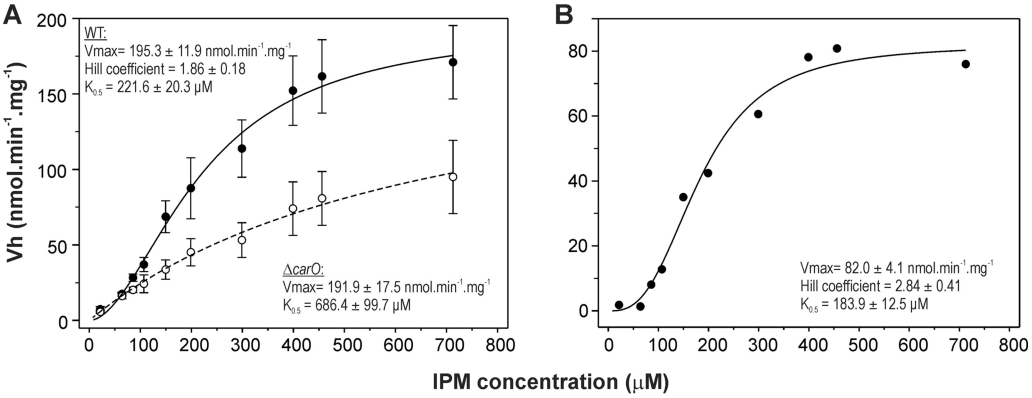

FIG 1 Kinetic analysis of IPM uptake by intact *A. baylyi* cells. (A) The IPM hydrolysis rates (V_h) of the WT and Δ*carO* mutants of *A. baylyi* (closed and open circles, respectively) at the indicated antibiotic concentrations were estimated using cells bearing pVIM. All assays were repeated at least three times, and the mean and standard deviation in each case are shown. (B) Further refinement of the analysis described for panel A to reflect the CarO contribution to IPM influx in which the mean V_h values of Δ*carO* mutant cells at each IPM concentration were subtracted from the equivalent values for WT cells. In both panels, the solid lines reflect sigmoidal fits obtained by using the three-parameter Hill equation, $y = y_{max} \times x^{\alpha}/(c^{\alpha} + x^{\alpha})$, and dashed lines indicate the hyperbolic fit using the single rectangular equation, $y = y_{max} \times x/(c + x)$. In all cases, y is the hydrolysis rate (V_h), x is the IPM concentration (μM), y_{max} is the V_{max} (nmol · min^{-1} · mg^{-1}), α is the Hill parameter coefficient, and c is $K_{0.5}$ (μM), the concentration of IPM at which $V_h = 0.5 \times V_{max}$ and also a measure of the affinity of the channel for the drug. The maximum IPM hydrolysis rates (obtained with equivalent amounts of disrupted cells) and the extent of VIM leakage (obtained with equivalent volumes of supernatants after removal of intact cells by centrifugation) at each antibiotic concentration are shown in Fig. S1 in the supplemental material.

other channels, and shed light on the possible roles of channel mutations in the evolution of carbapenem resistance in *Acinetobacter*.

(Parts of this research have been presented previously at different scientific meetings [43, 44].)

RESULTS

Kinetic analysis and comparison of IPM uptake by WT and Δ*carO* intact cells of *A. baylyi*. *A. baylyi* has been found to display higher levels of intrinsic susceptibility to IPM than to other β-lactams (9, 11), indicating an efficient uptake of IPM and thus providing a well-established model to characterize the type(s) of carbapenem channels present in the OM. We thus decided to characterize kinetically the process of IPM influx into intact *A. baylyi* cells for a more quantitative evaluation of these uptake sites, by following procedures frequently used for other Gram-negative bacteria (12, 36–39). In short, IPM uptake was coupled with a rapid "sink" process in the periplasm attained by a VIM-11 carbapenemase which was obtained by transforming the cells with plasmid pVIM (see Materials and Methods for details), and the initial IPM hydrolysis rates (V_h) by the cells were then determined at different concentrations of the carbapenem (Fig. 1 and see Fig. S1 in the supplemental material). Since we are especially interested in the roles of *Acinetobacter* CarO family members in the uptake of carbapenems and basic amino acids (13–15), we also constructed an *A. baylyi* Δ*carO* mutant in order to determine the kinetics of IPM permeation into these cells (see Materials and Methods and Fig. 6 below). Some control experiments (39) were conducted before considering that the reductions in V_h measured in wild-type (WT) and Δ*carO* cells reflected the limitation of the corresponding OM to IPM uptake and therefore the total rate of antibiotic influx (V_{in}) into the cells. We first verified that the levels of VIM-11 carbapenemase in these cells were sufficient to accurately measure the corresponding IPM steady-state hydrolysis rates for the antibiotic concentration range tested (Fig. S1). As shown in Fig. S1, the initial rates of IPM hydrolysis obtained from disrupted WT or Δ*carO* mutant cells were similar within the IPM concentration range assayed, thus indicating the presence of surplus VIM-11 carbapenemase. We then analyzed possible VIM leakage from these cells, a situation that would certainly affect the accuracy of uptake assays. As also shown in Fig. S1, the rates of IPM hydrolysis in supernatants obtained after removal of intact WT or Δ*carO* cells by centrifugation generally varied from nondetect-

able to less than 5% of the maximal values obtained from the corresponding disrupted cells, thus indicating very low VIM-11 leakage. We thus considered that the V_h values shown in Fig. 1 provide a good estimation of the rates of IPM uptake by the analyzed cells for the submillimolar IPM concentration range tested.

As shown in Fig. 1A, IPM influx into *A. baylyi* WT cells showed saturation at IPM concentrations close to 400 μM, with a best fit of the experimental data to a Hill model with a coefficient of 1.86 and an apparent $K_{0.5}$ for IPM of 221.6 $\pm$ 20.3 μM. The saturation kinetics observed at this IPM concentration range thus reinforce the existence of a specific channel(s) allowing uptake of this carbapenem in the *Acinetobacter* OM. It is noteworthy that significant IPM influx was also observed using Δ*carO* mutants (Fig. 1A) with signs of saturation observed at the higher IPM concentrations tested, with the experimental data fitting best in this case a hyperbolic plot with an apparent $K_{0.5}$ for IPM of 686.4 $\pm$ 99.7 μM. The latter result revealed the existence of a specific uptake site(s) for IPM other than CarO in the OM which, although apparently displaying relatively lower affinity for this carbapenem, may also be relevant in defining the rate of antibiotic influx into the cells at the concentration range tested.

To examine in more detail the contribution of CarO to IPM uptake, we conducted a further refinement of the above analysis in which the IPM influx rates of the Δ*carO* mutants were subtracted from those of WT cells at each IPM concentration tested (Fig. 1B). As shown in Fig. 1B, the results reinforced the notion that CarO provides a specific uptake site for IPM based on not only the saturation kinetics obtained but also the apparent cooperative behavior for this site from the best fit of the data to a Hill model with a coefficient of 2.84. It is worth noting that the apparent $K_{0.5}$ for IPM in CarO derived from this subtractive analysis (183.9 $\pm$ 12.5 μM) was comparable to that obtained for the specific OprD channel of *Pseudomonas aeruginosa* (36).

Overall, the above-described kinetic studies (i) reinforced the notion that CarO participates in the specific uptake of IPM through the *A. baylyi* OM and (ii) showed the existence of another specific site(s) displaying a relatively lower affinity for this carbapenem but potentially still involved in defining the rate of influx into the cells at submillimolar external antibiotic concentration ranges.

Basic amino acids compete with IPM for uptake into intact *A. baylyi* cells. Carbapenem β-lactams and basic amino acids share structural resemblances in parts of their molecules, which explains their common recognition by the specific site in the well-characterized *P. aeruginosa* OprD/OccD1 channel (6, 7, 10, 37, 45) (Fig. S2). These similarities include, besides an overall positive charge at pH values around 7, a carboxylate group at C-3 on the five-membered ring of the 4:5 fused bicyclic β-lactam backbone (the equivalent to the α-carboxylate group in the amino acid) separated by 6 to 7 bond lengths from a positively charged amino group located in the substituent bound at C-2 on the same ring (the equivalent to the second charged amino group at the basic amino acid side chain). For *P. aeruginosa* OprD/OccD1, some length variation between these two groups is allowed, since Lys, Arg, Orn, and 2,3-diaminopropionate (DAP), in which the separation between groups covers a range of 6 to 3 bond lengths, represented almost equally effective competitors of IPM entrance into the cells (37).

To obtain clues on the recognition abilities of the IPM channels of the *A. baylyi* OM, we next used competition studies of IPM uptake into whole cells by testing the competition ability afforded by Lys, Arg, Orn, and DAP among the basic amino acids. We also tested putrescine (i.e., 1,4-diaminobutane), glutamine, and Gly as potential competitors, some of them exemplifying compounds that share structural resemblances with basic amino acids in different sections of their molecules (32, 37). Based on the results shown in Fig. 1, we decided to employ a subsaturating concentration of IPM of 107 μM in these competition assays and to test all compounds at three different concentrations (0.1, 1, and 10 mM) to better evaluate their relative competition abilities. We also measured competition for IPM uptake compounds in both WT (Fig. 2, first [black] bars) and Δ*carO* mutant (Fig. 2, second [light gray] bars) cells, the latter not only to characterize the recognition abilities of the channel(s) other than CarO but also to

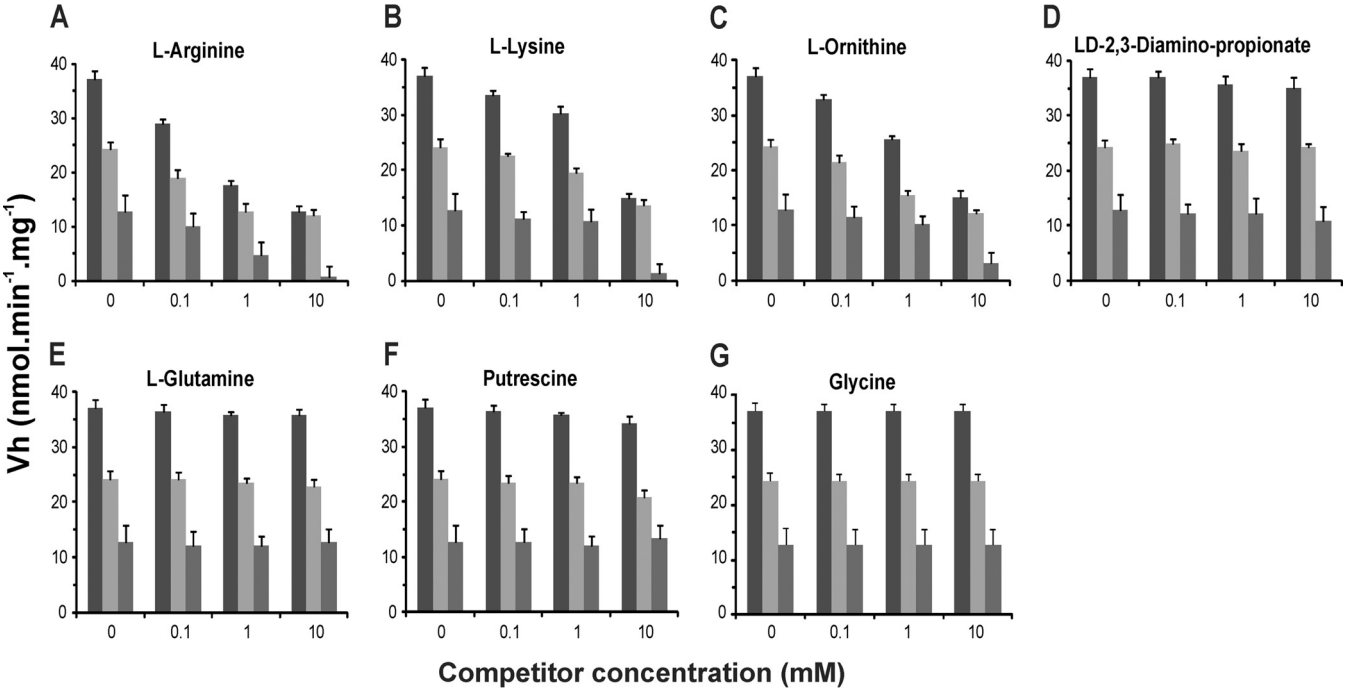

FIG 2 Effect of basic amino acids and related compounds on rates of IPM influx into *A. baylyi* WT and Δ*carO* mutant cells. The V_h values in the presence of 107 μM IPM in the absence (0) or presence of the indicated concentrations (0.1, 1, and 10 mM) of the different compounds tested were determined as described in Materials and Methods. At least three independent measurements were done for each condition, and the means and standard deviations are indicated. In all cases, the first (black) bars correspond to the values obtained for *A. baylyi* WT cells, the second (light gray) bars correspond to those of the Δ*carO* mutants, and the third (dark gray) bars correspond to the values obtained after subtracting the V_h of the Δ*carO* mutants from that of the WT cells under each independent condition.

better evaluate the contribution of CarO by subtracting the IPM influx values obtained for these mutants from the corresponding values for the WT cells (Fig. 2, third [dark gray] bars).

The overall results shown in Fig. 2 allowed us to draw the following conclusions. (i) Of the different compounds tested, only the basic amino acids Arg, Lys, and Orn were found to significantly compete for IPM uptake into both WT cells (first bars) and Δ*carO* mutants (second bars); the other compounds tested (e.g., DAP, glutamine, putrescine, and Gly) were largely ineffectual as competitors. The latter results not only reinforced the above notion of the existence of a specific channel(s) for IPM other than CarO in the *A. baylyi* OM (Fig. 1) but also indicated that these sites have recognition sites for basic amino acids. (ii) The subtractive analyses (Fig. 2A to G, third bars) may reveal in further detail the competition specifically afforded by each of the basic amino acids with IPM for uptake through CarO. Of them, Arg seemingly represented the most effective competitor (Fig. 2A to C), thus suggesting differential affinities of the CarO site for these basic amino acids. (iii) The near lack of competition afforded by putrescine to IPM uptake (Fig. 2F) strongly suggested that the α-carboxyl group in the basic amino acid is pivotal for recognition purposes by both CarO and the other specific site(s) of the *A. baylyi* OM and revealed similarities between the IPM-specific channels of *Acinetobacter* and *Pseudomonas* (see above). (iv) A similar conclusion might be drawn by the lack of competition shown by glutamine (Fig. 2E), suggesting that reductions in the electropositive character of the side chain amino group impaired recognition by the specific site(s) of the basic amino acids present in the *A. baylyi* OM, as occurred with *Pseudomonas* OprD (37). (v) DAP acted as an almost null competitor of IPM entrance into *A. baylyi* cells even at the higher concentration tested (Fig. 2D). This suggested that the length between the α-carboxyl and the side chain amino group is important for substrate recognition purposes by the IPM-specific site(s) of the *A. baylyi* OM and represented a differential feature from those of *P. aeruginosa* (37). (vi) Gly represented

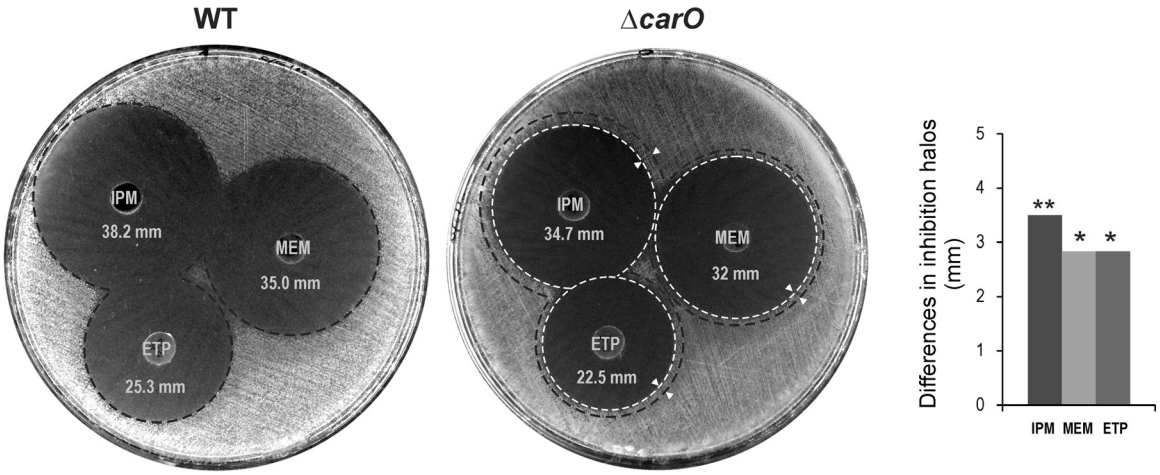

FIG 3 Susceptibility to different carbapenems of *A. baylyi* WT and Δ*carO* mutant cells. Representative results are shown of inhibition halos generated by IPM, meropenem (MPM), or ertapenem (ETP) disks containing 10 μg antibiotic each on *A. baylyi* WT (dashed black circles) or Δ*carO* mutant (dashed white circles) cells transformed with pVIM and growing on BM2/Glu solid medium supplemented with 30 μg/ml of chloramphenicol, and the corresponding diameters obtained in each case are indicated. In the figure corresponding to the Δ*carO* mutant, the inhibition halos for the WT strain have been superimposed (dashed black circles) for comparison purposes. The differences in inhibition halos between Δ*carO* mutants and the WT strain for a given carbapenem (limits depicted by white arrowheads) are shown in the graph on the right. The asterisks indicate the results of the statistical analysis (see Table S2 in the supplemental material). The reductions in inhibition zones were considered statistically significant when $0.001 < P < 0.01$ (**) and $0.01 < P < 0.05$ (*).

an almost null competitor of IPM uptake by either WT or Δ*carO* mutant cells under the conditions tested (Fig. 2G). Recent liposome swelling studies indicated that reconstituted *A. baumannii* CarO could mediate low-level uptake of Orn and also of Gly when tested at millimolar concentrations in the external medium (32). It should be noted, however, that OM-specific channels can allow the selective permeation of compounds for which no sites were detected by competition assays (7, 10, 46) and which could explain the apparent divergences between previous observations (32) and our observations described above using whole cells in the particular case of Gly.

It follows from the above-described results that at least two different uptake sites for IPM may be described in the *A. baylyi* OM. One site is represented by CarO, which showed characteristics of a saturable site in which basic amino acids specifically competed with IPM for uptake. In addition, these results uncovered the presence of a second uptake site for IPM displaying somewhat lower affinity for this carbapenem and also showing competition with basic amino acids.

Loss of CarO in *A. baylyi* impaired growth on Arg. Given the observations above, we next analyzed whether CarO could provide the *A. baylyi* cells with a specific uptake site for basic amino acids required for growth. From the different basic amino acids tested as potential carbon sources (Arg, His, Lys, and Orn), *A. baylyi* WT cells showed appreciable growth only on Arg although at a rate lower than those obtained in rich medium or in minimal medium using other carbon sources, including glutamate, citrate, and pyruvate (Table S4 and data not shown). Still, the loss of CarO specifically reduced *A. baylyi* growth on Arg, as reflected by the almost 60% reduction in growth rates found for the Δ*carO* mutants on 10 mM Arg in comparison to the WT cells (Table S4, experiment 1; see also Fig. 5A). These results support the notion that CarO provides *A. baylyi* with a specific uptake site for Arg, as occurred in the case of *A. baumannii* reported previously (15).

Loss of CarO in *A. baylyi* reduced cell susceptibility to carbapenems. We next analyzed the potential contributions of CarO loss to IPM resistance in *A. baylyi* by comparing the susceptibility phenotypes of WT and Δ*carO* mutant cells for different carbapenems, including IPM, meropenem (MPM), and ertapenem (ETP) (Fig. 3). Given the high carbapenem susceptibility of *A. baylyi* (MIC of 0.0625 μg/ml for IPM), we decided to use cells transformed with pVIM and therefore displaying increased carbapenem resistance (MIC of 12 μg/ml for IPM) (Tables S1 and S4) to amplify any effect

resulting from CarO loss to the susceptibility phenotype. The loss of CarO promoted only limited increments in the IPM resistance of pVIM-transformed cells, based on the increases in the MIC values from 12 μg/ml (WT) to 16 μg/ml (Δ*carO* mutants) (Table S1). Subtle reductions in carbapenem susceptibility of the Δ*carO* mutants were best observed by comparing the inhibition halos generated in agar diffusion tests by disks containing IPM, MPM, or ETP (Fig. 3; see also Table S2). In such tests, a gradient concentration for the antibiotic in the agar is experimentally obtained, with the highest concentration obtained near the disk and decreasing with distance until a limit in which no inhibitory concentration is reached (47, 48). Thus, the comparisons between the halos generated by the WT and the mutant strain may help reveal subtle reductions in susceptibility for each of these carbapenems resulting from the mutation, which are manifested at the limits of the antibiotic inhibitory concentration (48). As shown in Fig. 3 (see also Table S2), the Δ*carO* mutants consistently showed small but significant reductions in susceptibility for all three carbapenems in comparison to the susceptibility of the WT strain. Conversely, significant reductions in the susceptibility of the Δ*carO* mutants for other β-lactams, including piperacillin, cefoxitin, and cefepime, were not observed using similar antibiotic diffusion tests (not shown).

The results described above thus reinforced the notion that CarO provides a specific uptake site for carbapenems in the *A. baylyi* OM. The observation that the reductions in susceptibility are only modest (Fig. 3) further suggested the existence of another relevant specific site(s) allowing carbapenem uptake obtained from the kinetic studies (Fig. 1).

Carbapenem susceptibility of *A. baylyi* OM mutants lacking putative carbapenem channels. A limited number of *A. baumannii* OM proteins besides CarO have also been proposed to participate in the uptake of carbapenems on the basis of the loss or reduced expression of the proteins in different clinical *A. baumannii* strains (3, 16, 17). These include Omp33/36, whose loss has been associated with increased resistance to carbapenems and other β-lactams (16), and a 43-kDa OM protein designated OprD (17). *A. baumannii* OprD, recently also designated OccAB1, is part of the OM carboxylate channel (Occ) family and is similar to the well-known carbapenem-specific channel OprD/OccD1 of *P. aeruginosa*, sharing 29% identity and 49% similarity (25, 33). The role of OprD/OccAB1 in carbapenem uptake has recently been under scrutiny (25, 27). Moreover, recent liposome swelling studies with reconstituted *A. baumannii* OprD/OccAB1 indicated that this protein has general porin features similar to those of OmpF, allowing uptake of different compounds such as amino acids, carbohydrates, and antibiotics, including carbapenems and other β-lactams, when these compounds are present in the external medium at millimolar concentrations (33).

Since our results described above indicate the existence of a relevant specific site(s) other than CarO that allows carbapenem entrance in the *A. baylyi* OM, we analyzed whether individual *A. baylyi* ACIAD mutants (40) lacking homologs of Omp33/36 or OprD/OcAB1 showed alterations in carbapenem susceptibility (Fig. 4; see also Table S3). Comparative protein sequence analysis indicated that *A. baumannii* Omp33/36 (GenBank accession no. CAJ01528.1) (16) shares 92% identity and 98% overall similarity with its *A. baylyi* Omp34 homolog (GenBank accession no. CAG70110.1) and that *A. baumannii* OprD/OccAB1 (GenBank accession no. WP_000910001.1) (25) shares 63% identity and 75% overall similarity with its closest *A. baylyi* homolog (GenBank accession no. CAG67206).

As for the Δ*carO* mutants described above, moderate increments in IPM resistance for pVIM-transformed cells were observed only for the Δ*oprD* mutant of *A. baylyi*, based on the increments in MIC values in comparison to the corresponding WT strain (Table S1). Similar conclusions were drawn by measuring the inhibition halos for IPM, MPM, or ETP of Δ*omp34* and Δ*oprD* mutants, of which only the Δ*oprD* cells showed significant reductions in susceptibility, compared to the corresponding WT strains, to all of these carbapenems (Fig. 4; see also Table S3). Moreover, determinations of growth rates on rich medium and on minimal medium using glutamate as a carbon source (Table S4) indicated significant growth rate reductions only for the Δ*oprD* mutant. In addition, as

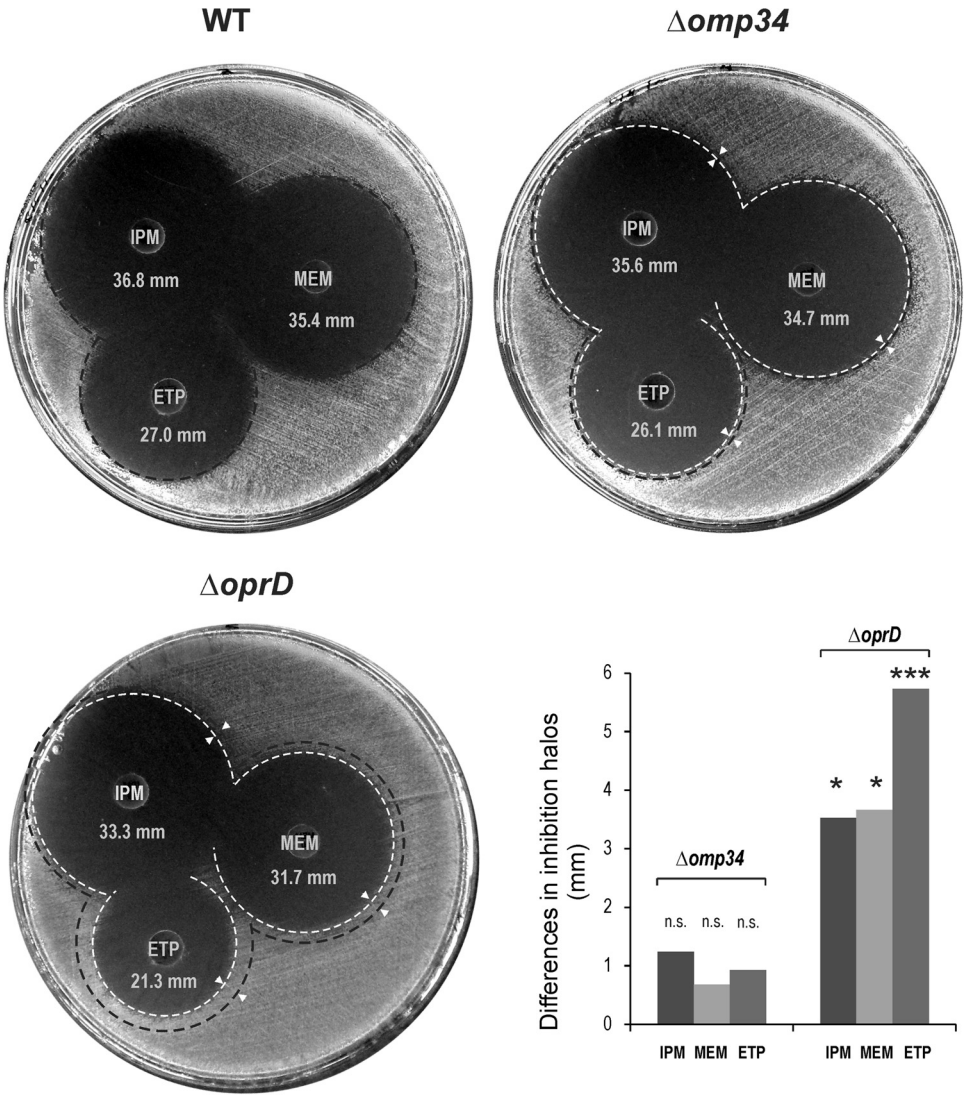

FIG 4 Susceptibility to different carbapenems of *A. baylyi* WT and selected OM mutants. Representative results are shown of inhibition halos generated by IPM, meropenem (MPM), or ertapenem (ETP) disks containing 10 μg antibiotic each on *A. baylyi* WT cells (dashed black circles) or Δ*omp34* or Δ*oprD* mutant cells (dashed white circles) from the ACIAD collection (40) transformed with pVIM growing on BM2/Glu solid medium supplemented with 30 μg/ml of chloramphenicol. For other details, see the legend to Fig. 3. The reductions in inhibition zones (see Table S3 in the supplemental material) were considered statistically significant when $0.0001 < P < 0.001$ (***), $0.001 < P < 0.01$ (**), and $0.01 < P < 0.05$ (*). n.s., nonsignificant.

shown in Table S4, this particular mutant was unable to grow on L-Arg as the only carbon source (see also Fig. 5B). The above-described situations are compatible with a proposed role for its *A. baumannii* OprD/OccAB1 homolog as an OM channel for glutamate and L-Arg, among other substrates (33).

As with CarO, the results described above point to OprD/OccAB1 as also representing a moderate uptake site for carbapenems in the *A. baylyi* OM. Since our results also indicated significant competition between these IPM uptake sites with L-Arg (Fig. 2), we next evaluated whether the loss of Omp34 or OprD/OccAB1 resulted in any effects on the growth of the corresponding *A. baylyi* mutants on this basic amino acid. As shown in Fig. 5B, only the Δ*oprD* mutants were largely impaired in growth in L-Arg, compared to other carbon sources such as glutamate, as occurred in the case of the Δ*carO* mutants (Fig. 5A). This reinforced the notion that OprD/OccAB1 may provide the cells with a second specific uptake site for basic amino acids that is also used by carbapenems to permeate the *Acinetobacter* OM.

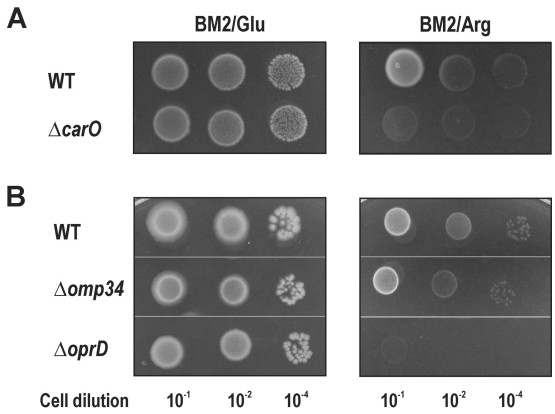

FIG 5 Growth of *A. baylyi* WT and selected OM protein mutants on L-Arg. The described WT or individual mutant cells were grown overnight at 30°C in BM2/Glu liquid medium, and 5-μl aliquots of 10-fold serial dilutions as indicated were plated on BM2 solid medium supplemented with L-glutamate (BM2/Glu) or L-arginine (BM2/Arg) at 10 mM each. The plates were incubated at 30°C for 24 h (BM2/Glu) and 72 h (BM2/Arg). The strains used are described in the legends to Fig. 3 and 4.

Further attempts were made to elucidate possible synergic actions on IPM uptake caused by the simultaneous removal of CarO and any of the above-mentioned proteins from the OM. For this purpose, Δ*omp34* Δ*carO* and Δ*oprD* Δ*carO* double mutants of *A. baylyi* were constructed as detailed in Materials and Methods. However, the significant increments in susceptibility to sodium dodecyl sulfate (SDS) observed for these double mutants (Fig. S3) indicated that although not sufficient to promote synthetic lethality, the function of the OM as a general permeability barrier was substantially impaired by the simultaneous loss of CarO and OprD or CarO and Omp34 in these cells. These observations are in concordance with the significant reductions in growth rates observed for the corresponding mutants, compared to those of the single mutants or the WT strain (Table S4), also indicating alterations in substrate uptake properties. These results precluded at this stage the study of possible synergic actions on IPM uptake resulting from the simultaneous removal of two proposed IPM channels from the *A. baylyi* OM.

DISCUSSION

The comparative kinetic and competition analyses of IPM uptake by *A. baylyi* whole cells conducted in this work allowed us to identify different uptake sites in the OM allowing for significant influx of carbapenems. One of them was represented by CarO, which showed saturable kinetics in the IPM submillimolar concentration range compatible with a specific uptake site (Fig. 1). Competition for IPM uptake in whole cells by different compounds further indicated that the CarO site could specifically recognize basic amino acids such as Arg, Lys, and Orn (Fig. 2). The *A. baylyi* Δ*carO* mutant was in fact impaired in growth on L-Arg in comparison to its growth on other carbon sources (Fig. 5; see also Table S4 in the supplemental material), reinforcing the previous notion (15) that CarO provides (or forms part of) a specific channel for basic amino acids in *Acinetobacter* species. Our studies also revealed the existence in the *A. baylyi* OM of an additional specific channel(s) with lower affinity for IPM (than that of CarO) displaying binding sites for basic amino acids (Fig. 2). Carbapenem susceptibility studies using other selected *A. baylyi* mutants pointed to OprD/OccAB1 as representing a second carbapenem-specific channel (Fig. 4), a result further supported by the observation that *A. baylyi* Δ*oprD* mutants were impaired in growth on L-Arg (Fig. 5 and Table S4).

The existence of different specific channels allowing for significant carbapenem uptake in the *A. baylyi* OM may help explain some of the difficulties in their identification in *A. baumannii* and the controversies about their roles (3, 14, 15, 18, 19, 24, 25, 27, 32, 33) and may provide clues for the understanding of the evolution of carbapenem resistance in this opportunistic pathogen. In a multiple-carbapenem-channel

scenario such as that envisaged here, the simultaneous loss of more than one uptake site would be required to significantly reduce carbapenem influx and therefore susceptibility. However, it is unlikely that the simultaneous selection of mutants in two different channels could occur, particularly if these channels serve specific roles in nutrient uptake. Therefore, in the context of carbapenem therapy pressure, another mechanism(s) of resistance such as the acquisition of β-lactamases with carbapenemase activity would be expected to be primarily selected, which seems to be the situation in *A. baumannii* (3). However, once the cells have acquired a main resistance mechanism, the selection of mutated variants on a given channel that promote even slight reductions in carbapenem permeation may still occur in selective antibiotic concentration windows in which small resistance differences may favor the growth of the mutants over the parental cells (8, 35, 48). By using antibiotic disk diffusion tests, we found that *A. baylyi* cells bearing deletions in *carO* or *oprD*, in particular, showed low reductions in susceptibility to IPM, MPM, and ETP (Fig. 3 and 4). This suggested that specific concentrations within the corresponding carbapenem gradients occurring near the limits of the inhibitory concentration for the WT strain may provide special environments for the selection of such mutants. These "resistance-selective compartments" are likely present at particular locations in the host during the course of antibiotic therapy (35, 48).

In the context of carbapenem therapy pressure, the multiple-carbapenem-channel scenario posed above would predict an increased frequency of mutations affecting *carO* integrity among *A. baumannii* strains already displaying a relatively robust mechanism of carbapenem resistance. In this context, other authors have reported the existence of insertion sequence (IS)-mediated disruptive events affecting *carO* (frequencies ranging from 3 to 14%) among epidemiologically related carbapenem-resistant *A. baumannii* clinical isolates in which the overproduction of diverse OXA enzymes represented the main mechanism of resistance (20–22, 26, 30, 31, 34, 49). It is worth noting that the simultaneous sequencing of Omp33/36 and OprD (21) or the sequencing of Omp33/36 (31) or OprD (49) of the isolates analyzed in the cited reports indicated no disruptive events affecting the corresponding genes. This suggests that while the complete loss of CarO can be tolerated by *A. baumannii* under carbapenem selection pressure, the simultaneous loss of CarO and OprD/OccAB1 may result in unattainable fitness costs in a situation compatible with a proposed role of the latter OM protein as a channel for multiple growth substrates (33) or with the ensuing defects in the barrier permeability functions of the OM (e.g., see Fig. S3 and Table S4). An alternative is represented by the replacement of either OM protein by variants displaying slightly reduced permeation/affinity for carbapenems, and in this context, we have previously shown the existence in the *A. baumannii* population of four well-defined *carO* allelic variants whose exchange is mediated by horizontal gene transfer (24). This suggests the possibility that noninactivating mutations in carbapenem channels other than CarO may eventually also emerge in *A. baumannii*, contributing in time to the stepwise reductions in the intrinsic susceptibility of this pathogen to these antibiotics.

CarO forms part of a novel family of OM proteins restricted to the *Moraxellaceae* family of the *Gammaproteobacteria*, which includes pathogenic species of the genera *Acinetobacter* and *Moraxella* (14). Therefore, the potential roles of CarO family members in the physiopathology of these organisms are worth studying in further detail (24, 32). In this context, OM channel roles in members of this family represent unexpected features for eight-stranded β-barrel proteins (7, 32). In fact, a number of controversies exist on whether the different *A. baumannii* CarO variants might provide channel functions for basic amino acids and/or carbapenems (14, 15, 18, 19, 32). Recent crystallographic studies using three recombinant *A. baumannii* CarO variants indicated that all of them refolded in similar monomeric eight-stranded β-barrel structures lacking an open channel in the crystal (32). However, these analyses also indicated that these proteins interacted preferentially with positively charged compounds and, most notably, that they could mediate a low but selective uptake of Orn when reconstituted in phospholipid bilayers (32). The overall experimental evidence from other laboratories

summarized above and the results presented in this work seem then to concur in that CarO family members can provide a recognition site for basic amino acids and even mediate their low-rate diffusion through the OM, although the exact mechanism is still obscure. There exist different alternatives which may overcome the limitations imposed by the relatively small size of these OM proteins. It seems feasible in principle that alternate CarO forms allowing the binding and diffusion of charged substrates are generated *in vivo*, and in this context the formation of low-abundance 10-β-stranded (or even 12-β-stranded) forms may not be completely excluded (32). However, monomeric forms may be insufficient to allow the permeation of the bulky carbapenems, and two other alternatives exist which could explain the participation of CarO in their uptake. One is that CarO assembles *in vivo* in oligomeric forms capable of accommodating larger compounds, a situation described for TolC family members which are structured as trimers in the OM with each protomer contributing to the formation of a wide-open channel (7). Another possibility is that rather than forming a channel by itself, CarO may serve as a specific receptor for positively charged compounds whose import through the OM then requires the recruiting of other OM proteins in a situation similar to that employed by colicins or certain vitamins (7, 50). We have previously noted the formation of large molecular structures containing CarO in the *A. baumannii* OM (24) which can represent either homo-oligomeric or hetero-oligomeric forms in a situation compatible with either of the two alternatives posed above.

Further work is in progress to elucidate the details of carbapenem uptake through the *Acinetobacter* OM and the identity and roles of the different OM proteins involved in this process.

MATERIALS AND METHODS

Bacterial strains and plasmids used in this work. *A. baylyi* ADP1 (1, 2) was kindly provided by L. N. Ornston (Department of Molecular, Cellular and Developmental Biology, Yale University, New Haven, CT, USA). The Δ*carO* mutant of this strain was constructed as described below. The *A. baylyi* ACIAD3459 (Δ*omp34*), ACIAD0240 (Δ*oprD*), and ACIAD0697 (Δ*ompA*) mutants and their corresponding wild-type (WT) strain (40) were kindly provided by Veronique de Berardinis, Genoscope/CEA, Evry Cedex, France. SDS-PAGE analysis of isolated OM fractions followed by Coomassie blue staining confirmed the loss of the corresponding OM proteins in these mutants (not shown).

***A. baylyi* culture conditions.** *A. baylyi* growth in liquid cultures was done at 30°C in either Luria-Bertani (LB) medium or BM2 minimal medium under aerobic conditions with vigorous shaking. BM2 basal medium (51) is composed of 62 mM potassium phosphate (pH 7.0), 7 mM $(NH_4)_2SO_4$, and 0.5 mM $MgSO_4$ and was supplemented with 10 μM $FeSO_4$ and the carbon sources at the concentrations indicated in the text. Solid medium incorporated 1.5% (wt/vol) Difco agar into the above-mentioned liquid media. Where indicated, 15 μg/ml kanamycin (Km), 30 μg/ml chloramphenicol (Cm), or 15 μg/ml of gentamicin (Gm) was added to the above-mentioned media.

Construction of an *A. baylyi* Δ*carO* mutant. The *A. baylyi* genome contains a *carO* family member whose product shares 68% identity and 84% overall similarity with *A. baumannii* CarO (14). *A. baylyi* CarO is effectively produced by the cells and represents the second most abundant OM protein after OmpA, as determined by SDS-PAGE/immunoblot analyses of OM fractions (Fig. 6), as in the case of *A. baumannii* (15, 24). The *A. baylyi carO* gene was replaced by an antibiotic cassette conferring kanamycin (*npt*) resistance derived from plasmid pBBR1MCS-2 (52). The *npt* gene was first amplified by PCR using primers Km_Fw (5′-AAGTGCGAATTCGGATGAATGTCAGCTAC-3′) and Km_Rv (5′-CCAGAGGAATTCTCAGAAGAACT CGTCAAG-3′) containing extra EcoRI sites (underlined), and the resulting fragment was digested with EcoRI and cloned into the equivalent site of pBlueScript SK(−) (53), thus generating pBS-npt. Two fragments of approximately 1 kbp, each containing the chromosomal regions located upstream of (Up) and downstream of (Dw) *A. baylyi carO*, were obtained by PCR amplification using primers CarO_UpFw (5′-GATAGTTCTAGAGGCTTGAAGTGGCTCAAG-3′) and CarO_UpRv (5′-GTACCTGGATCCGCACGAACACCTA CTG-3′) and primers CarO_DwFw (5′-AATGCAAAGCTTCAAAAGATCCGTAACG-3′) and CarO_DwRv (5′-GTCTGGGTCGACTAAACACATTAAAGA-3′), respectively, designed after the *A. baylyi* genome sequence information (http://www.genoscope.cns.fr/spip/Acinetobacter-baylyi-whole-genome.html). The primers incorporated additional restriction enzyme sites (TCTAGA, XbaI; GGATCC, BamHI; AAGCTT, HindIII; GTCGAC, SalI) that allowed cloning of the corresponding fragments into pBS-npt bordering the *npt* gene by taking advantage of the equivalent sites present in the multicloning site of the vector (53). The pBS-ΔcarO::npt plasmid thus obtained was used as a source of a linear DNA fragment of approximately 3 kbp in which the *npt* gene is bracketed by the immediate chromosomal fragments bordering *carO*. *A. baylyi* cells were transformed with this construction by taking advantage of their natural competence (1). After the cells were plated on solid LB medium containing Km and incubated for 48 h at 30°C, different Km-resistant clones were selected for subsequent analyses. The loss of CarO in the OM fractions of these cells was verified by SDS-PAGE and immunoblotting, and a selected Δ*carO* mutant was used for further analysis (Fig. 6). No significant impairment in growth on either rich medium (LB) or minimal BM2 medium

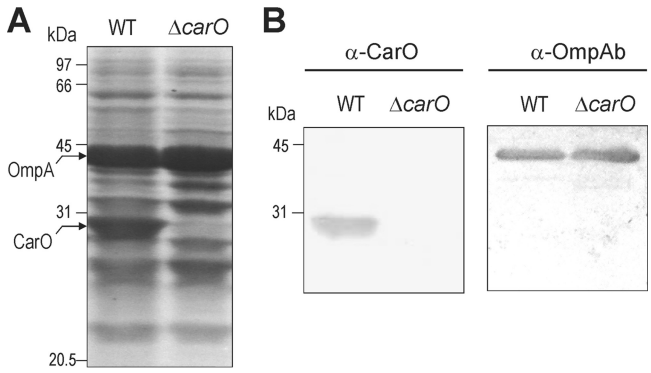

FIG 6 SDS-PAGE and immunoblot analyses of OM fractions of *A. baylyi* WT and Δ*carO* mutants. The equivalent of 20 μg of purified OM protein fractions of the indicated *A. baylyi* cells was subjected to SDS-PAGE, followed by staining with Coomassie blue (A) or immunoblotting with polyclonal rabbit antibodies toward *A. baumannii* CarO (α-CarO) or OmpAb (α-OmpAb) (B). The final positions of CarO and OmpA and the molecular mass markers in the gels are shown on the left of each panel. For details, see Materials and Methods.

containing 10 mM potassium glutamate (BM2/Glu) was observed for the *A. baylyi* Δ*carO* mutant, based on the growth rates obtained that were similar to those of WT cells (see Table S4 in the supplemental material). Also, no major alterations in OM permeability barrier functions against SDS were detected in these mutants, based on the similar SDS susceptibilities shown by Δ*carO* and WT cells when grown in solid LB medium containing 0.01 to 0.05% of this detergent (Fig. S3 and data not shown).

For the construction of Δ*omp34* Δ*carO* and Δ*oprD* Δ*carO* double mutants, the *npt* cassette in plasmid pBS-ΔcarO::npt (see above) was first replaced with a 0.8-kbp fragment containing the *aacC1* gene encoding gentamicin resistance. This generated pBS-ΔcarO::aacC1, in which the *aacC1* gene is now bracketed by the chromosomal fragments bordering *carO* and which was used to separately introduce the Δ*carO*::*aacC1* allele into the Km-resistant mutants ACIAD3459 (Δ*omp34*) and ACIAD0240 (Δ*oprD*) by following the procedures described above. After selection in LB solid medium containing 15 μg/ml Km and 15 μg/ml Gm, different colonies were tested in each case for the loss of CarO by immunoblot analysis with anti-CarO antibodies as described above. The Δ*omp34* Δ*carO* and Δ*oprD* Δ*carO* double mutants thus generated were evaluated for SDS susceptibility in comparison with the corresponding single mutants and the WT strain (Fig. S3).

Growth rate determinations. The growth rates of the different *A. baylyi* mutants and corresponding WT cells analyzed here in LB broth or liquid BM2 minimal medium supplemented with the indicated carbon sources (Table S4) were determined at 30°C under aerobic conditions and vigorous shaking. For this purpose, a seed culture grown overnight was diluted 1/100 in fresh culture medium and incubated as described above, and aliquots were withdrawn at different time intervals to determine the absorbance at 600 nm (A_{600}) to estimate the corresponding growth rates in accordance with standard procedures.

***A. baylyi* growth on amino acids as carbon sources.** The ability of the different *A. baylyi* mutants and corresponding WT cells analyzed here to use a given amino acid as a carbon source was tested as described for *A. baumannii* (15), using BM2 minimal medium supplemented with the indicated amino acids at the concentrations specified in tables or figure legends.

IPM uptake assays by intact *A. baylyi* cells. Quantitative estimations of the diffusion rates of IPM through the OM of intact *A. baylyi* cells were done by measuring the rate of IPM hydrolysis by cells containing a periplasmic VIM-11 carbapenemase essentially in accordance with previously described procedures (7, 36, 39). In short, WT or Δ*carO* mutant cells were first transformed with plasmid pVIM expressing the bla_{VIM-11} gene (54) and resistant clones were selected in LB agar plates containing 30 μg/ml Cm. The metallo-β-lactamase VIM-11 displays good catalytic efficiency for IPM hydrolysis, with K_m and k_{cat} values for the purified enzyme of 9.4 μM and 20 s^{-1}, respectively (54). The correct export and assembly of this enzyme into the *A. baylyi* periplasm were assessed by comparing the increases in MICs of IPM for *A. baylyi* cells bearing pVIM (12 μg/ml) with those for cells bearing the empty plasmid vector p$\alpha\Omega$ (0.0625 μg/ml). In addition, the amounts of VIM-11 produced by WT and Δ*carO* mutant cells transformed with pVIM were similar, based on SDS-PAGE and immunoblot analyses with anti-VIM (Fig. S1).

To assay IPM uptake by whole cells, WT or Δ*carO* mutants bearing pVIM were grown at 30°C in LB broth containing 30 μg/ml Cm to an A_{600} of 0.6. At this stage, the cells were harvested by centrifugation at 1,500 $\times$ *g* for 20 min at 4°C, rinsed twice with an ice-cold solution of 10 mM HEPES (pH 7.5)–200 mM NaCl–5 mM $MgSO_4$, resuspended in the same medium to an A_{600} of 0.2, and kept on ice until measurements were made. The initial rates of IPM hydrolysis (V_h) were measured spectrophotometrically at 30°C by following the decrease in A_{300} at each IPM concentration in a final volume of 1 ml of resuspension medium. A Jasco V-630 UV-VIS spectrophotometer and quartz cuvettes with a 10-mm path length were used for this purpose. The total rates of IPM hydrolysis were measured on cell aliquots after sonic disruption to release all VIM imipenemase into the medium by using equivalent cell volumes. The extent of VIM leakage from intact cells into the medium was measured using the supernatants of equivalent cell volumes after centrifugation at 1,500 $\times$ *g* for 10 min.

β-Lactam susceptibility assays. Where indicated, the MICs for IPM (Table S1) were determined by the agar dilution method employing Mueller-Hinton agar (MHA) in accordance with CLSI-recommended procedures (55). Intermediate MIC values were determined by using the appropriate IPM dilutions. To best evaluate differences in susceptibility between *A. baylyi* WT and Δ*carO* mutant cells to carbapenems, we compared the corresponding inhibition zones generated by the diffusion from disks containing the tested antibiotics (47) on bacteria growing on minimal agar medium. In short, the analyzed strains were grown overnight at 30°C in liquid BM2/Glu medium, and aliquots of these cultures were diluted with BM2 basal medium to a turbidity corresponding to 0.5 McFarland units. The suspensions were spread on the surfaces of petri plates containing BM2/Glu agar medium and other additions specified in the figure legends. Antimicrobial disks containing 10 μg of the indicated β-lactams (BBL Sensi-Disc; Becton Dickinson and Company, Sparks, MD, USA) were carefully deposited on the center of the agar surface, and the plates were subsequently incubated at 30°C for 24 h. The diameters of the growth inhibition zones on several replicates were measured to evaluate the effects of a particular mutation on the susceptibility of the analyzed cells to a given β-lactam. MHA was not employed for this purpose to reduce possible interferences exerted by the free basic amino acid content of this rich medium (56).

SDS-PAGE and immunoblot analyses of *A. baylyi* OM fractions. Whole *A. baylyi* cells or the corresponding OM fractions were analyzed by SDS-PAGE using 12% (wt/vol) polyacrylamide gels in accordance with protocols previously described for *A. baumannii* (14, 15, 24). Where indicated, immunoblot analyses were conducted using rabbit polyclonal antibodies against *A. baumannii* CarO (14, 15, 24), OmpAb (12), or VIM-2 (the latter kindly provided by R. Bonomo and A. Vila). Determinations of protein contents in the different OM fractions were done by a modified Lowry procedure incorporating 0.1% SDS to solubilize membrane proteins as described previously (14).

SUPPLEMENTAL MATERIAL

Supplemental material for this article may be found at https://doi.org/10.1128/AAC.01737-16.

TEXT S1, PDF file, 0.5 MB.

ACKNOWLEDGMENTS

We are indebted to L. N. Ornston (Department of Molecular, Cellular and Developmental Biology, Yale University, New Haven, CT, USA) for providing the *A. baylyi* ADP1 strain used to construct the Δ*carO* mutant described in this work, V. de Berardinis (Genoscope/CEA, Evry Cedex, France) for her generous gift of different *A. baylyi* ACIAD mutants of the Genoscope collection, and R. Bonomo (Research Service, Louis Stokes Cleveland Department of Veterans Affairs Medical Center, Cleveland, OH, USA) and A. Vila (IBR, Rosario) for providing the rabbit anti-VIM-2 antibodies. We also thank M. A. Mussi for her help with mutant construction and O. Roveri and N. Carrillo (Department of Biological Chemistry, Facultad de Ciencias Bioquímicas y Farmacéuticas, UNR) for their generous help in kinetic analyses and for critically reading the manuscript.

This work was supported by grants from Agencia Nacional de Promoción Científica y Tecnológica (ANPCyT; PICT-2011-1020), CONICET (PIP 1055), and Ministerio de Ciencia, Tecnología e Innovación Productiva, Provincia de Santa Fe, Argentina.

V.R. is a former Fellow of ANPCyT, L.B. and M.M.C. are Fellows of CONICET, A.M.V. and J.M.-B. are Career Researchers of CONICET, and A.S.L. is a Researcher of the UNR.

REFERENCES

1. Young DM, Parke D, Ornston LN. 2005. Opportunities for genetic investigation afforded by *Acinetobacter baylyi*, a nutritionally versatile bacterial species that is highly competent for natural transformation. Annu Rev Microbiol 59:519–551. https://doi.org/10.1146/annurev.micro.59.051905.105823.
2. Vaneechoutte M, Young DM, Ornston LN, De BT, Nemec A, Van Der Reijden T, Carr E, Tjernberg I, Dijkshoorn L. 2006. Naturally transformable *Acinetobacter* sp. strain ADP1 belongs to the newly described species *Acinetobacter baylyi*. Appl Environ Microbiol 72:932–936. https://doi.org/10.1128/AEM.72.1.932-936.2006.
3. Roca I, Espinal P, Vila-Farres X, Vila J. 2012. The *Acinetobacter baumannii* oxymoron: commensal hospital dweller turned pan-drug-resistant menace. Front Microbiol 3:148. https://doi.org/10.3389/fmicb.2012.00148.
4. Antunes LC, Visca P, Towner KJ. 2014. *Acinetobacter baumannii*: evolution of a global pathogen. Pathog Dis 71:292–301. https://doi.org/10.1111/2049-632X.12125.
5. Averhoff B. 2015. *Acinetobacter baumannii*—understanding and fighting a new emerging pathogen. Environ Microbiol Rep 7:6–8. https://doi.org/10.1111/1758-2229.12224.
6. Papp-Wallace KM, Endimiani A, Taracila MA, Bonomo RA. 2011. Carbapenems: past, present, and future. Antimicrob Agents Chemother 55:4943–4960. https://doi.org/10.1128/AAC.00296-11.
7. Nikaido H. 2003. Molecular basis of bacterial outer membrane permeability revisited. Microbiol Mol Biol Rev 67:593–656. https://doi.org/10.1128/MMBR.67.4.593-656.2003.
8. Fernandez L, Hancock RE. 2012. Adaptive and mutational resistance: role of porins and efflux pumps in drug resistance. Clin Microbiol Rev 25:661–681. https://doi.org/10.1128/CMR.00043-12.
9. Gomez MJ, Neyfakh AA. 2006. Genes involved in intrinsic antibiotic resistance of *Acinetobacter baylyi*. Antimicrob Agents Chemother 50:3562–3567. https://doi.org/10.1128/AAC.00579-06.
10. Isabella VM, Campbell AJ, Manchester J, Sylvester M, Nayar AS, Ferguson KE, Tommasi R, Miller AA. 2015. Toward the rational design of carbap-

enem uptake in *Pseudomonas aeruginosa*. Chem Biol 22:535–547. https://doi.org/10.1016/j.chembiol.2015.03.018.
11. Beceiro A, Perez-Llarena FJ, Perez A, Tomas MM, Fernandez A, Mallo S, Villanueva R, Bou G. 2007. Molecular characterization of the gene encoding a new AmpC beta-lactamase in *Acinetobacter baylyi*. J Antimicrob Chemother 59:996–1000. https://doi.org/10.1093/jac/dkm070.
12. Sugawara E, Nikaido H. 2012. OmpA is the principal nonspecific slow porin of *Acinetobacter baumannii*. J Bacteriol 194:4089–4096. https://doi.org/10.1128/JB.00435-12.
13. Limansky AS, Mussi MA, Viale AM. 2002. Loss of a 29-kilodalton outer membrane protein in *Acinetobacter baumannii* is associated with imipenem resistance. J Clin Microbiol 40:4776–4778. https://doi.org/10.1128/JCM.40.12.4776-4778.2002.
14. Mussi MA, Limansky AS, Viale AM. 2005. Acquisition of resistance to carbapenems in multidrug-resistant clinical strains of *Acinetobacter baumannii*: natural insertional inactivation of a gene encoding a member of a novel family of beta-barrel outer membrane proteins. Antimicrob Agents Chemother 49:1432–1440. https://doi.org/10.1128/AAC.49.4.1432-1440.2005.
15. Mussi MA, Relling VM, Limansky AS, Viale AM. 2007. CarO, an *Acinetobacter baumannii* outer membrane protein involved in carbapenem resistance, is essential for L-ornithine uptake. FEBS Lett 581:5573–5578. https://doi.org/10.1016/j.febslet.2007.10.063.
16. del Mar Tomás M, Beceiro A, Perez A, Velasco D, Moure R, Villanueva R, Martinez-Beltran J, Bou G. 2005. Cloning and functional analysis of the gene encoding the 33- to 36-kilodalton outer membrane protein associated with carbapenem resistance in *Acinetobacter baumannii*. Antimicrob Agents Chemother 49:5172–5175. https://doi.org/10.1128/AAC.49.12.5172-5175.2005.
17. Dupont M, Pages JM, Lafitte D, Siroy A, Bollet C. 2005. Identification of an OprD homologue in *Acinetobacter baumannii*. J Proteome Res 4:2386–2390. https://doi.org/10.1021/pr050143q.
18. Siroy A, Molle V, Lemaitre-Guillier C, Vallenet D, Pestel-Caron M, Cozzone AJ, Jouenne T, De E. 2005. Channel formation by CarO, the carbapenem resistance-associated outer membrane protein of *Acinetobacter baumannii*. Antimicrob Agents Chemother 49:4876–4883. https://doi.org/10.1128/AAC.49.12.4876-4883.2005.
19. Catel-Ferreira M, Coadou G, Molle V, Mugnier P, Nordmann P, Siroy A, Jouenne T, De E. 2011. Structure-function relationships of CarO, the carbapenem resistance-associated outer membrane protein of *Acinetobacter baumannii*. J Antimicrob Chemother 66:2053–2056. https://doi.org/10.1093/jac/dkr267.
20. Lu PL, Doumith M, Livermore DM, Chen TP, Woodford N. 2009. Diversity of carbapenem resistance mechanisms in *Acinetobacter baumannii* from a Taiwan hospital: spread of plasmid-borne OXA-72 carbapenemase. J Antimicrob Chemother 63:641–647. https://doi.org/10.1093/jac/dkn553.
21. Lee Y, Kim CK, Lee H, Jeong SH, Yong D, Lee K. 2011. A novel insertion sequence, IS*Aba10*, inserted into IS*Aba1* adjacent to the *bla*(OXA-23) gene and disrupting the outer membrane protein gene *carO* in *Acinetobacter baumannii*. Antimicrob Agents Chemother 55:361–363. https://doi.org/10.1128/AAC.01672-09.
22. He C, Xie Y, Fan H, Kang M, Tao C, Zhang R, Hu Y, Chen Z, Wang L. 2011. Spread of imipenem-resistant *Acinetobacter baumannii* of European clone II in Western China. Int J Antimicrob Agents 38:257–260. https://doi.org/10.1016/j.ijantimicag.2011.04.015.
23. Luo L, Jiang X, Wu Q, Wei L, Li J, Ying C. 2011. Efflux pump overexpression in conjunction with alternation of outer membrane protein may induce *Acinetobacter baumannii* resistant to imipenem. Chemotherapy 57:77–84. https://doi.org/10.1159/000323620.
24. Mussi MA, Limansky AS, Relling V, Ravasi P, Arakaki A, Actis LA, Viale AM. 2011. Horizontal gene transfer and assortative recombination within the *Acinetobacter baumannii* clinical population provide genetic diversity at the single *carO* gene, encoding a major outer membrane protein channel. J Bacteriol 193:4736–4748. https://doi.org/10.1128/JB.01533-10.
25. Catel-Ferreira M, Nehme R, Molle V, Aranda J, Bouffartigues E, Chevalier S, Bou G, Jouenne T, De E. 2012. Deciphering the function of the outer membrane protein OprD homologue of *Acinetobacter baumannii*. Antimicrob Agents Chemother 56:3826–3832. https://doi.org/10.1128/AAC.06022-11.
26. Fonseca EL, Scheidegger E, Freitas FS, Cipriano R, Vicente AC. 2013. Carbapenem-resistant *Acinetobacter baumannii* from Brazil: role of *carO* alleles expression and *bla*OXA-23 gene. BMC Microbiol 13:245. https://doi.org/10.1186/1471-2180-13-245.
27. Smani Y, Pachon J. 2013. Loss of the OprD homologue protein in *Acinetobacter baumannii*: impact on carbapenem susceptibility. Antimicrob Agents Chemother 57:677. https://doi.org/10.1128/AAC.01277-12.
28. Smani Y, Dominguez-Herrera J, Pachon J. 2013. Association of the outer membrane protein Omp33 with fitness and virulence of *Acinetobacter baumannii*. J Infect Dis 208:1561–1570. https://doi.org/10.1093/infdis/jit386.
29. Rumbo C, Tomas M, Fernandez ME, Soares NC, Carvajal M, Santillana E, Beceiro A, Romero A, Bou G. 2014. The *Acinetobacter baumannii* Omp33-36 porin is a virulence factor that induces apoptosis and modulates autophagy in human cells. Infect Immun 82:4666–4680. https://doi.org/10.1128/IAI.02034-14.
30. Khorsi K, Messai Y, Hamidi M, Ammari H, Bakour R. 2015. High prevalence of multidrug-resistance in *Acinetobacter baumannii* and dissemination of carbapenemase-encoding genes *bla*OXA-23-like, *bla*OXA-24-like and *bla*NDM-1 in Algiers hospitals. Asian Pac J Trop Med 8:438–446. https://doi.org/10.1016/j.apjtm.2015.05.011.
31. Novovic K, Mihajlovic S, Vasiljevic Z, Filipic B, Begovic J, Jovcic B. 2015. Carbapenem-resistant *Acinetobacter baumannii* from Serbia: revision of CarO classification. PLoS One 10:e0122793. https://doi.org/10.1371/journal.pone.0122793.
32. Zahn M, D'Agostino T, Eren E, Basle A, Ceccarelli M, van den Berg B. 2015. Small-molecule transport by CarO, an abundant eight-stranded beta-barrel outer membrane protein from *Acinetobacter baumannii*. J Mol Biol 427:2329–2339. https://doi.org/10.1016/j.jmb.2015.03.016.
33. Zahn M, Bhamidimarri SP, Basle A, Winterhalter M, van den Berg B. 2016. Structural insights into outer membrane permeability of *Acinetobacter baumannii*. Structure 24:221–231. https://doi.org/10.1016/j.str.2015.12.009.
34. Sen B, Joshi SG. 2016. Studies on *Acinetobacter baumannii* involving multiple mechanisms of carbapenem resistance. J Appl Microbiol 120:619–629. https://doi.org/10.1111/jam.13037.
35. Negri MC, Lipsitch M, Blazquez J, Levin BR, Baquero F. 2000. Concentration-dependent selection of small phenotypic differences in TEM beta-lactamase-mediated antibiotic resistance. Antimicrob Agents Chemother 44:2485–2491. https://doi.org/10.1128/AAC.44.9.2485-2491.2000.
36. Trias J, Dufresne J, Levesque RC, Nikaido H. 1989. Decreased outer membrane permeability in imipenem-resistant mutants of *Pseudomonas aeruginosa*. Antimicrob Agents Chemother 33:1202–1206. https://doi.org/10.1128/AAC.33.8.1202.
37. Trias J, Nikaido H. 1990. Protein D2 channel of the *Pseudomonas aeruginosa* outer membrane has a binding site for basic amino acids and peptides. J Biol Chem 265:15680–15684.
38. Huang H, Hancock RE. 1996. The role of specific surface loop regions in determining the function of the imipenem-specific pore protein OprD of *Pseudomonas aeruginosa*. J Bacteriol 178:3085–3090. https://doi.org/10.1128/jb.178.11.3085-3090.1996.
39. Kojima S, Nikaido H. 2013. Permeation rates of penicillins indicate that *Escherichia coli* porins function principally as nonspecific channels. Proc Natl Acad Sci U S A 110:E2629–E2634. https://doi.org/10.1073/pnas.1310333110.
40. de Berardinis V, Vallenet D, Castelli V, Besnard M, Pinet A, Cruaud C, Samair S, Lechaplais C, Gyapay G, Richez C, Durot M, Kreimeyer A, Le FF, Schachter V, Pezo V, Doring V, Scarpelli C, Medigue C, Cohen GN, Marliere P, Salanoubat M, Weissenbach J. 2008. A complete collection of single-gene deletion mutants of *Acinetobacter baylyi* ADP1. Mol Syst Biol 4:174. https://doi.org/10.1038/msb.2008.10.
41. de Berardinis V, Durot M, Weissenbach J, Salanoubat M. 2009. *Acinetobacter baylyi* ADP1 as a model for metabolic system biology. Curr Opin Microbiol 12:568–576. https://doi.org/10.1016/j.mib.2009.07.005.
42. Elliott KT, Neidle EL. 2011. *Acinetobacter baylyi* ADP1: transforming the choice of model organism. IUBMB Life 63:1075–1080. https://doi.org/10.1002/iub.530.
43. Mussi MA, Relling VR, Ravasi P, Limansky AS, Viale AM. 2007. Functions of outer membrane protein CarO homolog in *Acinetobacter baylyi*, abstr P67, p 67. Abstr 43rd Annu Meet Argentine Soc Biochem Mol Biol, Mar del Plata, Argentina.
44. Relling VR, Limansky AS, Moran-Barrio J, Mussi MA, Brambilla L, Viale AM. 2013. Functional characterization of the *Acinetobacter baylyi* outer membrane CarO homolog as a channel for basic amino acids and imipenem in intact bacterial cells, abstr P3-32, p 75. Abstr 9th Int Symp Biol Acinetobacter, Cologne, Germany.
45. Eren E, Vijayaraghavan J, Liu J, Cheneke BR, Touw DS, Lepore BW, Indic M, Movileanu L, van den Berg B. 2012. Substrate specificity within a

family of outer membrane carboxylate channels. PLoS Biol 10:e1001242. https://doi.org/10.1371/journal.pbio.1001242.
46. Huang H, Hancock RE. 1993. Genetic definition of the substrate selectivity of outer membrane porin protein OprD of *Pseudomonas aeruginosa*. J Bacteriol 175:7793–7800. https://doi.org/10.1128/jb.175.24.7793-7800.1993.
47. Murray PR, Baron EJ, Jorgensen JH, Landry ML, Pfaller MA (ed). 2007. Manual of clinical microbiology, 9th ed. American Society for Microbiology, Washington, DC.
48. Baquero F, Coque TM. 2014. Widening the spaces of selection: evolution along sublethal antimicrobial gradients. mBio 5:e02270. https://doi.org/10.1128/mBio.02270-14.
49. Yang H, Huang L, Barnie PA, Su Z, Mi Z, Chen J, Aparna V, Kumar D, Xu H. 2015. Characterization and distribution of drug resistance associated beta-lactamase, membrane porin and efflux pump genes in MDR *A. baumannii* isolated from Zhenjiang, China. Int J Clin Exp Med 8:15393–15402.
50. Cascales E, Buchanan SK, Duche D, Kleanthous C, Lloubes R, Postle K, Riley M, Slatin S, Cavard D. 2007. Colicin biology. Microbiol Mol Biol Rev 71:158–229. https://doi.org/10.1128/MMBR.00036-06.
51. Gilleland HE, Jr, Stinnett JD, Eagon RG. 1974. Ultrastructural and chemical alteration of the cell envelope of *Pseudomonas aeruginosa*, associated with resistance to ethylenediaminetetraacetate resulting from growth in a $Mg2^{+}$-deficient medium. J Bacteriol 117:302–311.
52. Kovach ME, Elzer PH, Hill DS, Robertson GT, Farris MA, Roop RM, Peterson KM. 1995. Four new derivatives of the broad-host-range cloning vector pBBR1MCS, carrying different antibiotic-resistance cassettes. Gene 166:175–176. https://doi.org/10.1016/0378-1119(95)00584-1.
53. Sambrook J, Fitsch EF, Maniatis T. 1989. Molecular cloning: a laboratory manual. Cold Spring Harbor Laboratory Press, Cold Spring Harbor, NY.
54. Marchiaro P, Tomatis PE, Mussi MA, Pasteran F, Viale AM, Limansky AS, Vila AJ. 2008. Biochemical characterization of metallo-beta-lactamase VIM-11 from a *Pseudomonas aeruginosa* clinical strain. Antimicrob Agents Chemother 52:2250–2252. https://doi.org/10.1128/AAC.01025-07.
55. Clinical and Laboratory Standard Institute. 2006. Methods for dilution antimicrobial susceptibility tests for bacteria that grow aerobically, 7th ed. Approved standard M7-A7. Clinical and Laboratory Standards Institute, Wayne, PA.
56. Fukuoka T, Masuda N, Takenouchi T, Sekine N, Iijima M, Ohya S. 1991. Increase in susceptibility of Pseudomonas aeruginosa to carbapenem antibiotics in low-amino-acid media. Antimicrob Agents Chemother 35:529–532.